The Astrophysical Journal, 669:1050–1057, 2007 November 10

AN H_2CO 6 cm MASER PINPOINTING A POSSIBLE CIRCUMSTELLAR TORUS IN IRAS 18566+0408

E. Araya,[1,2] P. Hofner,[1,2] M. Sewiło,[3] W. M. Goss,[2] H. Linz,[4] S. Kurtz,[5]
L. Olmi,[6,7] E. Churchwell,[3] L. F. Rodríguez,[5] and G. Garay[8]
Received 2007 February 14; accepted 2007 July 6

ABSTRACT

We report observations of 6 cm, 3.6 cm, 1.3 cm, and 7 mm radio continuum, conducted with the Very Large Array, toward IRAS 18566+0408, one of the few sources known to harbor H_2CO 6 cm maser emission. Our observations reveal that the emission is dominated by an ionized jet at centimeter wavelengths. *Spitzer* IRAC images from GLIMPSE support this interpretation, given the presence of 4.5 μm excess emission at approximately the same orientation as the centimeter continuum. The 7 mm emission is dominated by thermal dust from a flattened structure almost perpendicular to the ionized jet; thus, the 7 mm emission appears to trace a torus associated with a young massive stellar object. The H_2CO 6 cm maser is coincident with the center of the torus-like structure. Our observations rule out radiative pumping via radio continuum as the excitation mechanism for the H_2CO 6 cm maser in IRAS 18566+0408.

Subject headings: H II regions — ISM: individual (IRAS 18566+0408) — ISM: molecules — masers — stars: formation

1. INTRODUCTION

How massive stars ($M > 10\,M_\odot$) form is among the most important unsolved problems in astrophysics. Large observational and theoretical efforts in the last 10 years support the hypothesis that massive stars form via accretion of material through disks; however, other possible mechanisms, such as spherical accretion and coalescence, cannot be discarded, mainly in the case of stars more massive than 20 $M_\odot$ (e.g., Beuther et al. 2007; Cesaroni et al. 2007; Beltrán et al. 2006). Evidence for massive star formation via accretion disks is mainly indirect; e.g., through the detection of jets and bipolar molecular outflows (e.g., Arce et al. 2007; Garay et al. 2003, 2007); however, more direct evidence, such as flattened rotating structures around young massive stellar objects, has been observed toward a number of objects (for example, see the review by Cesaroni et al. 2007). In some cases, CH_3OH, H_2O, SiO, and OH masers have also been reported to trace circumstellar disks around young massive stellar objects (e.g., see reviews by Cesaroni et al. 2007; Fish 2007).

Although the formation mechanism of massive stars is still not well understood, the sites where massive stars are being (or have been recently) formed are readily identifiable by the effects that young massive stellar objects have on their environments. Among such effects are massive molecular outflows, the formation of H II regions, and hot molecular cores, as well as the presence of maser emission from several molecular transitions (e.g., Churchwell 2002). The 6 cm *K*-doublet line of formaldehyde (H_2CO) is one of the molecular transitions that has been detected as maser emission toward massive star-forming regions. H_2CO 6 cm masers have several characteristics that distinguish them from other astrophysical masers: (1) they have been found toward a small number of regions (e.g., Araya et al. 2004, 2007b; Mehringer et al. 1995; Pratap et al. 1994; Forster et al. 1985), (2) they are weaker than other astrophysical masers, such as H_2O, OH, and CH_3OH masers (e.g., Araya et al. 2007b, 2007c; Hoffman et al. 2003, 2007), and (3) H_2CO masers have been only detected close to very young massive stellar objects (such as hot molecular cores and deeply embedded infrared sources; e.g., Araya et al. 2006) and appear not to be associated with high-velocity outflows or more evolved phases of massive star formation, such as compact H II regions (see review article by Araya et al. 2007a).

As pointed out by Mehringer et al. (1995), the paucity of H_2CO 6 cm masers suggests that the pumping mechanism of the masers may require quite specific physical conditions for the inversion, conditions that may be short-lived in massive star formation environments (see Araya et al. [2007a] for a discussion of other reasons why H_2CO masers may be rare). If this were the case, then H_2CO 6 cm masers could become a useful probe for the detection of specific physical conditions; however, at present there exists no model that can successfully explain H_2CO 6 cm masers. Although infrared and collisional excitation mechanisms have been discussed in the literature as agents capable of inverting the H_2CO 6 cm levels (see Litvak 1970; Thaddeus 1972), only Boland & de Jong (1981) developed a model specifically intended to explain one of the known H_2CO 6 cm maser sources, i.e., the maser in NGC 7538. Their model is based on radiative pumping of the H_2CO 6 cm levels by radio continuum from a background compact (emission measure [EM] of $>10^8$ pc cm^{-6}) H II region.

Araya et al. (2005) explored whether the Boland & de Jong (1981) model is capable of explaining the H_2CO 6 cm maser in IRAS 18566+0408, but they could not draw a strong conclusion due to insufficient observational constraints on the radio continuum properties of IRAS 18566+0408. Thus, to more critically test whether a pumping mechanism by radio continuum can explain the H_2CO maser in IRAS 18566+0408, and to explore the relation between the H_2CO maser and the massive star formation process in the region, we conducted a multiwavelength study of the radio continuum in IRAS 18566+0408. In § 1.1 we summarize the properties of IRAS 18566+0408; our observations and data

[1] Department of Physics, New Mexico Institute of Mining and Technology, Socorro, NM 87801.
[2] National Radio Astronomy Observatory, Socorro, NM 87801.
[3] Department of Astronomy, University of Wisconsin-Madison, Madison, WI 53706.
[4] Max-Planck-Institut für Astronomie, D-69117 Heidelberg, Germany.
[5] Centro de Radioastronomía y Astrofísica, Universidad Nacional Autónoma de México, 58089 Morelia, Michoacán, Mexico.
[6] Istituto di Radioastronomia, INAF, Sezione di Firenze, I-50125 Florence, Italy.
[7] Department of Physics, University of Puerto Rico at Rio Piedras, P.O. Box 23343, San Juan, PR 00931.
[8] Departamento de Astronomía, Universidad de Chile, Casilla 36-D, Santiago, Chile.

TABLE 1
VLA Observations

Parameter	C Band (6 cm)	X Band (3.6 cm)	K Band (1.3 cm)	Q Band (7 mm)
Date	2005 May 18	2005 May 18	2005 Aug 5	2003 Apr 25
VLA configuration	B	B	C	D
ν_0 (GHz)	4.86	8.46	22.46	43.34
R.A.[a]	18 59 09.9	18 59 09.9	18 59 10.0	18 59 09.9
Decl.[a]	04 12 10	04 12 10	04 12 14	04 12 14
Flux density calibrator	3C 286	3C 286	3C 286	3C 286
Assumed S_ν (Jy)	7.49	5.21	2.52	1.45
Phase calibrator	J1824+107	J1824+107	J1851+005	J1851+005
Measured S_ν (Jy)	0.77	0.72	0.97	0.66

Note.—Units of right ascension are hours, minutes, and seconds, and units of declination are degrees, arcminutes, and arcseconds.
[a] Phase tracking center (J2000.0).

reduction procedure are reported in § 2; and the results and discussion of the radio continuum observations are presented in § 3. In § 4 we report our conclusions.

1.1. *IRAS 18566+0408: A Massive Disk Candidate with an* H_2CO *Maser*

Located at a distance of 6.7 kpc, IRAS 18566+0408 (G37.55+0.20; Mol 83; Molinari et al. 1996) is a massive star-forming region with a bolometric luminosity of $\sim 6 \times 10^4\ L_\odot$, equivalent to the luminosity of an O8 ZAMS star (Sridharan et al. 2002; Araya et al. 2005).[9] Current star formation in the region is evident from the presence of multiple molecular outflows, as well as 22 GHz H_2O and 6.7 GHz CH_3OH maser emission (Beuther et al. 2002a, 2002b). Zhang et al. (2007) found that roughly all the far-IR luminosity comes from a single compact ($<5''$) source, indicating the presence of an embedded massive protostar.

IRAS 18566+0408 is an ideal source for the study of massive star formation because only a single weak radio continuum source is found in interferometric observations (Carral et al. 1999; Araya et al. 2005), and thus the study of the region is less susceptible to confusion. The absence of strong radio continuum indicates that IRAS 18566+0408 is in a phase prior to the development of a bright ultracompact H II region. IRAS 18566+0408 also harbors one of the few known H_2CO 6 cm masers in the Galaxy (Araya et al. 2005).

Zhang (2005) listed IRAS 18566+0408 as a massive circumstellar disk candidate. According to Zhang (2005), the massive disk[10] has a physical size of 8000 AU and a mass of 60 $M_\odot$. Zhang et al. (2007) have recently published a multifrequency study of IRAS 18566+0408. In § 3.3 we discuss their results in the context of the observations reported in this paper.

2. OBSERVATIONS AND DATA REDUCTION

We report VLA[11] radio continuum observations of IRAS 18566+0408 in the C (6 cm), X (3.6 cm), K (1.3 cm), and Q (7 mm) bands. The C- and X-band observations were carried out on 2005 May 18, with the VLA in the B configuration. The K- and Q-band observations were conducted on 2005 August 5 and 2003 April 25 with the VLA in the C and D configurations, respectively. The default VLA continuum mode (4IF; 50 MHz per IF) was used for the observations.

The total integration time on-source was approximately 1.6, 1.0, 1.9, and 0.5 hr for the C-, X-, K-, and Q-band observations, respectively. The observations were conducted in phase-referencing mode, with switching cycles (source/calibrator) of 720/120, 600/150, 120/40, and 50/50 s for the C-, X-, K-, and Q-band observations, respectively. We used the fast-switching VLA observing mode for the K- and Q-band observations, given that short calibration cycles are required to track rapid phase variations due to tropospheric instabilities.

The data reduction was conducted following the VLA high-frequency recipe for calibration and standard imaging procedures using the NRAO package AIPS. In Table 1 we give the details of the observations.

3. RESULTS AND DISCUSSION

We detected radio continuum emission from IRAS 18566+0408 at all observed wavelengths. In Figure 1 we show the images obtained in the different bands. In the figure we also mark the position of the H_2CO 6 cm maser (R.A. $= 18^h59^m09.975^s \pm 0.002^s$, decl. $= +04^\circ12'15.57'' \pm 0.03''$, J2000.0; Araya et al. 2005). In Table 2 we list the details of the radio images and the parameters of the continuum emission in IRAS 18566+0408.

3.1. *An* H_2CO 6 cm *Maser Pinpointing a Possible Circumstellar Torus*

In Figure 2 we show the radio spectral energy distribution (SED) of IRAS 18566+0408 based on our observations plus the 2 cm detection by Araya et al. (2005). We found that the SED is satisfactorily fitted by the combination of optically thin thermal dust emission plus optically thin bremsstrahlung radiation from an ionized jet. The dust emission in Figure 2 was fitted with the assumption of a dust temperature of 50 K; i.e., approximately the temperature of the warm dust component reported by Sridharan et al. (2002), and a dust opacity κ_ν that is proportional to $\lambda^{-1.8}$ (with $\kappa_{43.3\ \mathrm{GHz}} = 0.044\ \mathrm{cm^2\ g^{-1}}$) that was obtained from a fit of the opacities for dust particles with thin ice mantles and $n_{H_2} = 10^6\ \mathrm{cm^{-3}}$, presented by Ossenkopf & Henning (1994). Our assumption of κ_ν being proportional to $\lambda^{-\beta}$, where $\beta = 1.8$, is consistent with the recent empirical determination of β by Hill et al. (2006) for dust at 50 K.

Although the centimeter emission can be also well fitted by free-free radiation from a simple spherical H II region (see § 3.2), we decided to fit the centimeter emission using an ionized jet model, given the elongated morphology of the 6 cm and 3.6 cm continuum emission (Fig. 1); specifically, we used the "standard" collimated

[9] Recently, Zhang et al. (2007) estimated a total luminosity of $\sim 8 \times 10^4\ L_\odot$, mainly on the basis of mid- to far-IR data at $\sim 1'$ resolution.

[10] In this paper we use the term "massive disk" as synonymous with "circumstellar torus" (also referred as pseudodisks in the literature; Cesaroni et al. 2007). The term "massive disk" should not be confused with "accretion disk."

[11] The Very Large Array (VLA) is operated by the National Radio Astronomy Observatory (NRAO), a facility of the National Science Foundation operated under cooperative agreement by Associated Universities, Inc.

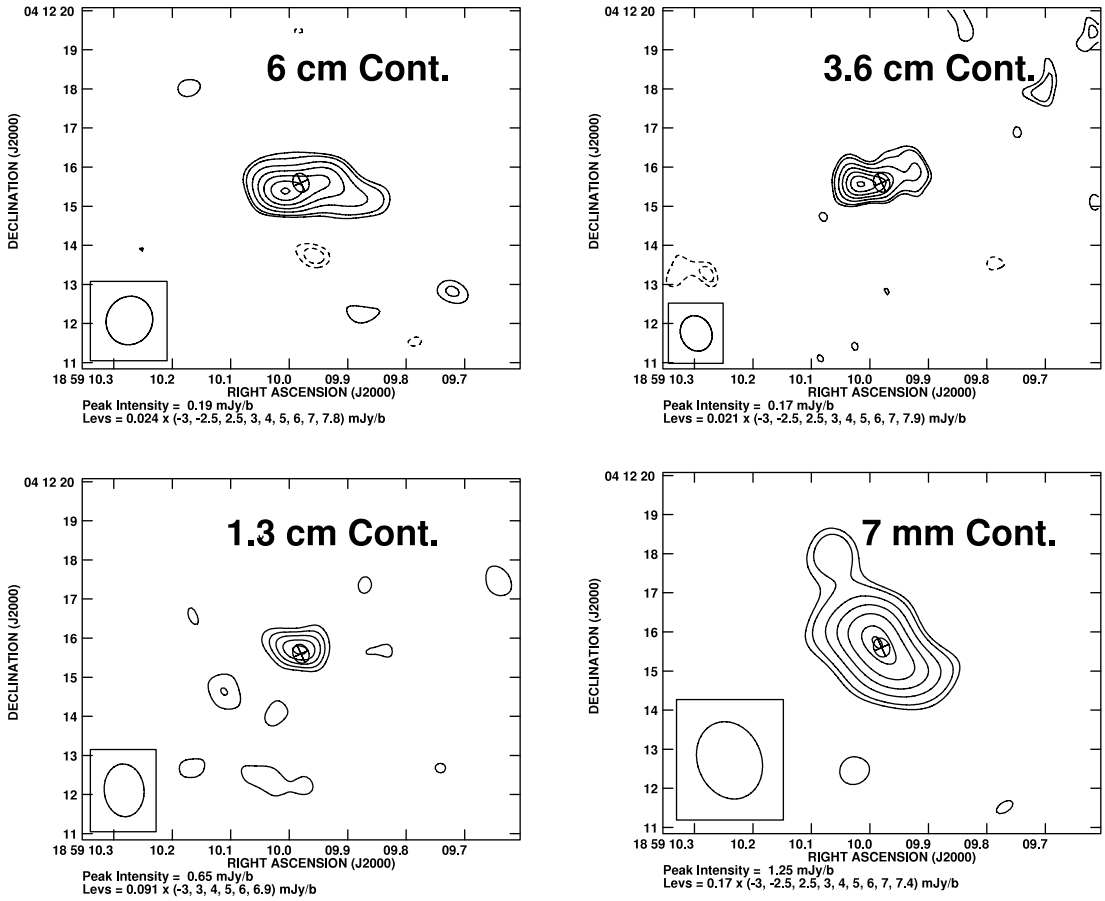

FIG. 1.—Radio continuum emission detected toward IRAS 18566+0408 at the four different wavelengths observed with the VLA. In the lower left corner of each image we show the respective synthesized beam (the size and position angle of the synthesized beams are given in Table 2). The location of the H_2CO 6 cm maser imaged with the A configuration of the VLA by Araya et al. (2005) is indicated by the $\oplus$ symbol. The size and position angle of the $\oplus$ symbol represent the size and position angle of the synthesized beam of the Araya et al. (2005) observations.

model of Reynolds (1986). The fit was obtained with the assumptions of an electron density of 2×10^4 cm^{-3} at 1340 AU (i.e., 0.2″ at 6.7 kpc) from the protostar, an electron temperature of 10^4 K, fully ionized gas, a width at the base of the jet of 1340 AU, and a half-length of the ionized jet of 6700 AU. In addition, we assumed that the jet is in the plane of the sky. The estimated ionized mass-loss rate is greater than $10^{-6}\ M_\odot$ yr^{-1} (if we assume a jet velocity of >100 km s^{-1}), which, for example, is comparable to the mass-loss rate of the ionized jet in GGD 27 (Martí et al. 1995). The overall centimeter-millimeter SED of IRAS 18566+0408 is very similar in shape, but much more luminous, when compared to those found in some low-mass young stars (e.g., L1551 IRS5; Rodríguez et al. 1998). Since we only detected optically thin radio emission from the jet, we cannot discriminate between different Reynolds models; i.e., by adjusting the parameters, all models can produce good fits. Thus, we are unable to precisely determine physical parameters of the ionized gas, such as the electron temperature and density.

The interpretation that the elongation detected at 6 cm and 3.6 cm is caused by an ionized jet is strengthened by *Spitzer* IRAC data of IRAS 18566+0408 from GLIMPSE. In Figure 3 we show a three-color image of IRAS 18566+0408 in the 3.6 μm (*blue*),

TABLE 2
PARAMETERS OF THE RADIO CONTINUUM IMAGES

Parameter	C Band (6 cm)	X Band (3.6 cm)	K Band (1.3 cm)	Q Band (7 mm)
Synthesized beam (arcsec)	1.3 × 1.2	0.93 × 0.79	1.4 × 1.0	2.0 × 1.6
Synthesized beam P.A. (deg)	−27	24	5	22
rms (μJy beam^{-1})	24	21	91	168
S_ν[a] (mJy)	0.52 ± 0.09	0.55 ± 0.10	0.80 ± 0.18	3.1 ± 0.6
Peak R.A.[a]	18 59 09.97 ± 0.01	18 59 09.99 ± 0.01	18 59 09.98 ± 0.01	18 59 09.99 ± 0.01
Peak decl.[a]	04 12 15.49 ± 0.08	04 12 15.67 ± 0.08	04 12 15.74 ± 0.06	04 12 15.70 ± 0.20
Deconvolved size[a] (arcsec)	2.9 × 0.73	2.3 × 0.85	<1.5 × 1.5	3.3 × 1.6
Deconvolved size P.A.[a] (deg)	85	103	...	45
Physical size (10^3 AU)	19 × 5	16 × 6	<10 × 10	22 × 11

NOTE.—Units of right ascension are hours, minutes, and seconds, and units of declination are degrees, arcminutes, and arcseconds.
[a] Parameters obtained from a two-dimensional Gaussian fit of the brightness distribution, using the task JMFIT in AIPS.

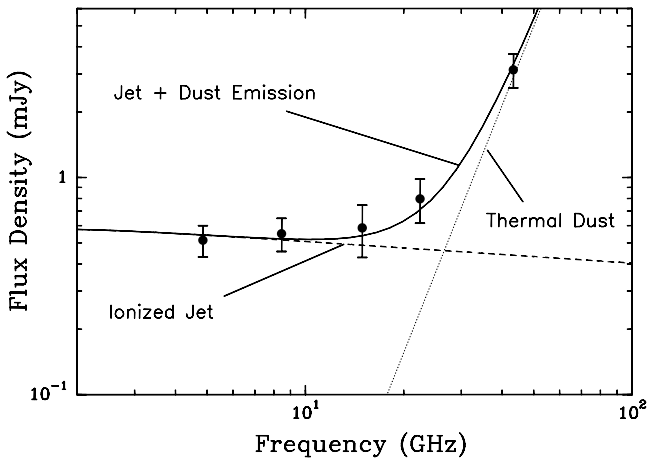

FIG. 2.—Radio SED of IRAS 18566+0408 based on the observations reported in this paper (Table 2), in addition to the 2 cm data point by Araya et al. (2005). The dashed line shows the fit to the ionized gas emission using the "standard" collimated ionized jet model developed by Reynolds (1986). At millimeter wavelengths the SED is dominated by optically thin thermal dust emission. The total fit to the SED, i.e., the addition of the ionized gas and thermal dust flux density, is shown with a solid line.

4.5 μm (*green*), and 8.0 μm (*red*) bands. The *Spitzer* data show an excess at 4.5 μm toward the northwest of the IRAS 18566+0408 position. Excess in the 4.5 μm band is a known tracer of outflows (shocked gas) in massive star-forming regions due to the contribution of H_2 emission lines (e.g., Noriega-Crespo et al. 2004; Smith et al. 2006). Thus, the similar orientation of the 4.5 μm excess and the centimeter radio continuum supports the interpretation that the elongation observed at 6 cm and 3.6 cm is due to an ionized jet.

In Figure 4 we show a three-color image of the 6 cm (*blue*), 3.6 cm (*green*), and 7 mm (*red*) emission as shown in Figure 1. The ionized jet is elongated in an approximately east-west orientation, and although the signal-to-noise ratio of the Q-band detection is low ($\sim 7\,\sigma$), the orientation of the 7 mm source (after beam deconvolution) is in the northeast-southwest direction. Since the 7 mm emission is almost perpendicular to the ionized jet and is dominated by thermal dust, it appears that the 7 mm source traces a circumstellar torus in IRAS 18566+0408. In Figure 4 we also show the location of the H_2CO 6 cm maser (Araya et al. 2005). The maser is coincident with the center of the torus-like structure.

Using the 7 mm dust flux density from the fit (Fig. 2), if we assume a 7 mm dust opacity of $\kappa_{43.3\ \mathrm{GHz}} = 0.044\ \mathrm{cm^2\ g^{-1}}$, a gas-to-dust ratio of 100, and a dust temperature of 50 K, the mass of the 7 mm source is $\sim 500\ M_\odot$ (if the gas temperature is 100 K,

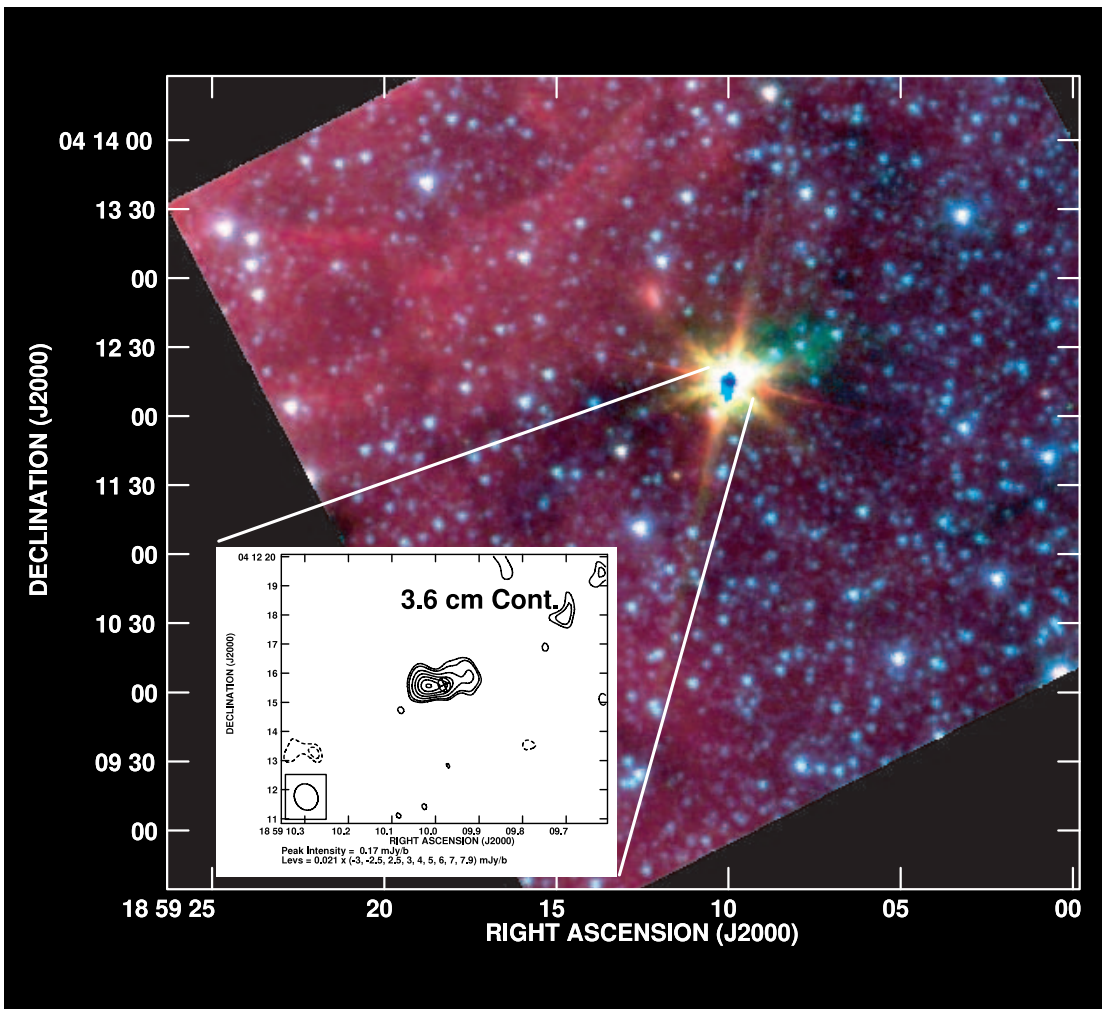

FIG. 3.—Three-color image of IRAS 18566+0408 from the *Spitzer* IRAC 3.6 μm (*blue*), 4.5 μm (*green*), and 8.0 μm (*red*) bands. The IRAC detectors were saturated at the IRAS 18566+0408 peak. Note the 4.5 μm (*green*) excess toward the northwest of IRAS 18566+0408. Excess in the 4.5 μm band is a known tracer of shocked gas in massive star-forming regions (e.g., Smith et al. 2006). In the inset we show the 3.6 cm radio image obtained here (see Fig. 1). The elongation of the 3.6 cm continuum source is approximately parallel to the 4.5 μm northwest excess, which agrees with the suggestion that the ionized gas traces a jet in IRAS 18566+0408.

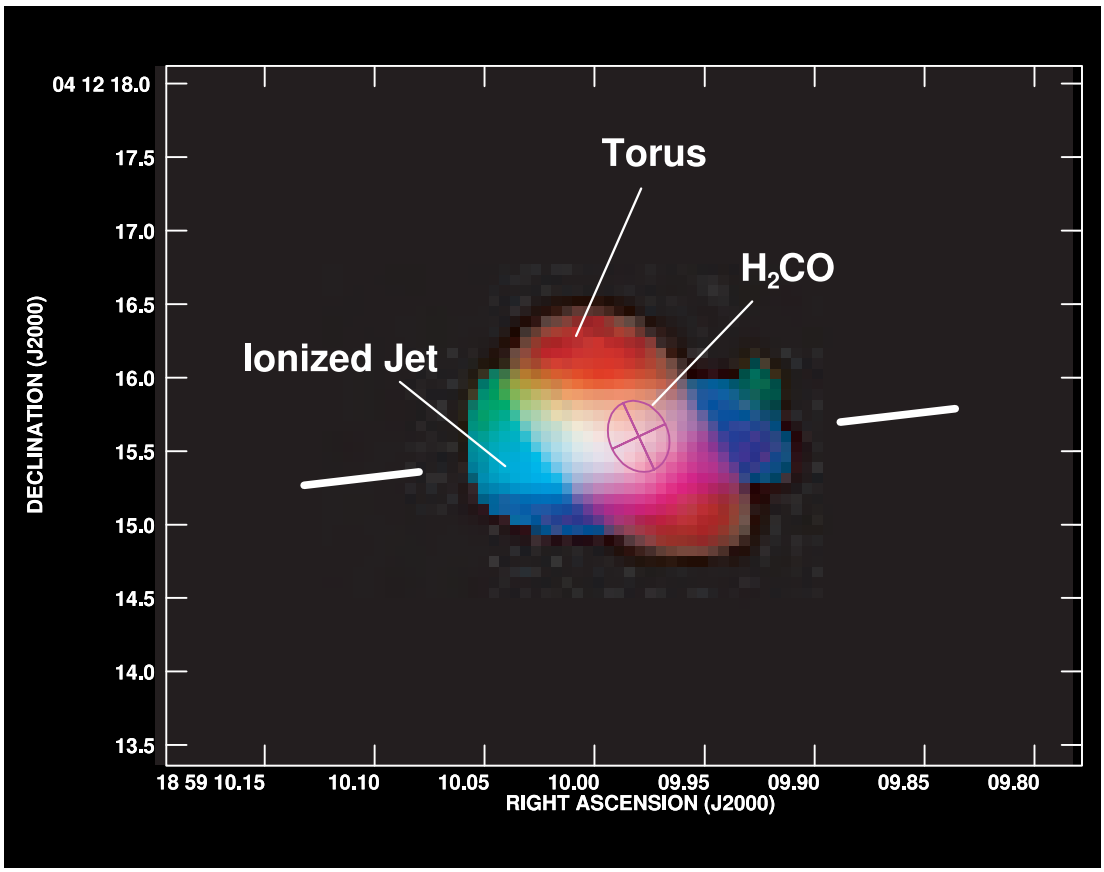

FIG. 4.—Three-color image of the 6 cm (*blue*), 3.6 cm (*green*), and 7 mm (*red*) radio continuum emission from IRAS 18566+0408. The colors were saturated to increase contrast. At centimeter wavelengths (where the emission is dominated by ionized gas), the brightness distribution is oriented east-west (highlighted by thick white lines), whereas at 7 mm the orientation is northeast-southwest. Given that the 7 mm emission is dominated by thermal dust and the ionized jet is almost perpendicular to the 7 mm source, the 7 mm flattened structure appears to trace a circumstellar torus. The H_2CO maser position as detected by Araya et al. (2005) is shown by the $\oplus$ symbol. The maser is coincident with the center of the 7 mm source.

the mass would be a factor of 2 smaller). Thus, the 7 mm source is indeed tracing a *massive* flattened structure. This torus candidate appears to be more massive and greater than the parameters reported by Zhang (2005; see, however, § 3.3). Our mass determination should be considered a rough estimate because of the uncertainties in the assumed gas-to-dust ratio, dust opacity, and dust temperature values. Nevertheless, we find that the mass of the 7 mm source must be larger than 10 $M_\odot$, since even after assuming an extremely large 7 mm dust opacity ($\kappa_{43.3\ \mathrm{GHz}} = 0.78\ \mathrm{cm^2\ g^{-1}}$; Rodríguez et al. 2007), the mass is still >10 $M_\odot$. If we assume that a single O8 ZAMS star is forming in IRAS 18566+0408 and that the torus mass is >10 $M_\odot$, then the $M_{\mathrm{star}}/M_{\mathrm{torus}}$ ratio for the system would be <2, suggesting that the torus-like structure is dynamically unstable (e.g., see Rodríguez et al. 2007 and references therein). Further high angular resolution observations of the region are needed to investigate the stability and kinematics of the 7 mm source.

3.2. *Applicability of the Boland & de Jong (1981) Model*

To test whether population inversion by radio continuum radiation can explain the H_2CO maser in IRAS 18566+0408, we adapted the Boland & de Jong (1981) formalism to the specific characteristics of IRAS 18566+0408. In particular, we included the contribution of dust emission to the photon occupation number,[12] and we used the following expression for the optical depth of the radio continuum emission (see Reynolds 1986):

$$\tau_\nu(y) = 2a_k w_0 n_0^2 x_0^2 T_0^{-1.35} (y/y_0)^{q_\tau} \nu^{-2.1}, \quad (1)$$

where $a_k = 0.212$, $q_\tau = -2$ for the "standard" collimated model of Reynolds (1986), $w_0 = 670$ AU, $n_0 = 2 \times 10^4$ cm^{-3}, $x_0 = 1$, and $T_0 = 10^4$ K (see § 3.1). We assumed that the ionized jet is in the plane of the sky (i.e., $\sin i = 1$ in the Reynolds [1986] notation; see also Fig. 1 in Reynolds 1986), and hence y is simply the distance along the ionized jet and y_0 is the distance at which the flow is injected (we assumed $y_0 = 1340$ AU on the basis of the IRAS 18566+0408 centimeter emission images; see Fig. 1).

Given the observational constraints imposed by our data, we find that the model does not predict population inversion of the 6 cm K-doublet level. The specific ionized gas model used to fit the centimeter radio continuum is not relevant to the outcome of the maser model as long as the free-free emission is optically thin at $\lambda \leq 6$ cm, as observed. For example, the centimeter SED of IRAS 18566+0408 can be fitted by optically thin emission from a cylindrical H II region characterized by $n_e = 1.7 \times 10^3$ cm^{-3}, $T_e = 10^4$ K, and EM $= 1.4 \times 10^5$ pc cm^{-6}. No inversion is predicted for such a background H II region (see discussion of Fig. 1 in Boland & de Jong [1981] and Fig. 4 in Araya et al. [2005]). We conclude that excitation by radio continuum is not a feasible mechanism with which to explain the maser in IRAS 18566+0408.

[12] In the case of NGC 7538, Boland & de Jong (1981) neglected dust emission because they considered that free-free radio continuum radiation was dominant at all wavelengths of interest.

3.3. *Comparison with the Observations by Zhang et al. (2007)*

Recently, Zhang et al. (2007) reported a multiwavelength study of IRAS 18566+0408. They conducted 22, 43, and 87 GHz radio continuum observations, as well as NH_3(1,1), (2,2), and (3,3), SiO(2–1), and HCN(1–0) observations with the VLA and the Owens Valley Radio Observatory. In this section we discuss the consistency of the results found in our work with respect to the results found by Zhang et al. (2007).

3.3.1. *A Jetlike Outflow in IRAS 18566 +0408*

The SiO(2–1) observations by Zhang et al. (2007) reveal a well-collimated molecular outflow in IRAS 18566+0408. The outflow appears to be emanating from the torus-like structure reported in this work. The SiO outflow is in the southeast-northwest direction, which is consistent with the orientation of the ionized jet and the large-structure outflow traced by *Spitzer* (see Figs. 3 and 4). However, the SiO outflow is not strictly collinear to the ionized jet or the 4.5 μm excess emission: within $\sim 1''$ from the center of the torus-like structure (Fig. 4), the ionized jet appears to have a position angle of $\sim 100^\circ$; at $\sim 10''$ from the torus, the position angle of the SiO outflow is 135°; and at $\sim 1'$ scales, the 4.5 μm outflow has a position angle of $\sim 110^\circ$. Given that the velocity gradient of the SiO outflow is opposite that of the CO outflow, Zhang et al. (2007) mentioned that the outflow may be very close to the plane of the sky and that the velocity inversion may be due to precession. The change in position angle between the radio jet, the SiO outflow, and the 4.5 μm outflow may also be due to precession of the jet.

The NH_3 and HCN data reported by Zhang et al. (2007) show an elongation parallel to the SiO outflow, indicating that these molecules may also be tracing the outflow. The NH_3(1,1) and (2,2) velocity-integrated emission is distributed almost symmetrically with respect to the center of the torus candidate, whereas the SiO, NH_3(3,3), and HCN integrated emission is elongated mostly toward the northwest of the 7 mm source. The asymmetry of the SiO, NH_3(3,3), and HCN emission with respect to the position of the torus-like structure is similar to that shown by the *Spitzer* 4.5 μm excess, in which 4.5 μm excess emission is only detected toward the northwest of the radio continuum source. Density gradients in the medium may be responsible for such an asymmetry.

3.3.2. *Continuum Observations*

Zhang et al. (2007) conducted continuum observations at 22, 43, and 87 GHz. At 87 GHz ($\theta_{\rm syn} \sim 5''$) they detected a continuum source coincident with the weak radio continuum source reported by Carral et al. (1999) and Araya et al. (2005; see also Fig. 1). The peak intensity of the emission is 18 mJy beam^{-1}, and the total flux density of the source is 31 mJy. The 87 GHz flux is clearly dominated by dust emission, which is consistent with our radio SED interpretation. Zhang et al. (2007) detected a second millimeter source (MM-2) northwest from the position of the protostellar candidate (see their Fig. 1). We did not detect a counterpart of MM-2 in our observations, which is consistent with the nondetection at 43 GHz by Zhang et al. (2007).

The 43 GHz observations reported by Zhang et al. (2007) were conducted with the VLA in the DnC configuration, resulting in a synthesized beam of $2.7'' \times 1.3''$, which is more elongated than our $\theta_{\rm syn}$ at 43 GHz (Table 2). The observations of Zhang et al. (2007) have a smaller rms than that of our observations; i.e., 0.1 versus 0.17 mJy beam^{-1}. As in our observations, they also detected 43 GHz emission coincident with the radio continuum source. The source is slightly resolved, with a peak intensity of 1 mJy beam^{-1} and a flux density of 1.7 mJy. The deconvolved size of the emission is $2.0'' \times 1.2''$, with a P.A. $= 24^\circ$, which corresponds to a major axis of 1.3×10^4 AU. Thus, the 7 mm source detected by Zhang et al. (2007) appears to be more compact, and the emission appears to be weaker than the 7 mm emission reported in this work (Table 2). To investigate the origin of this discrepancy, we reduced the 7 mm observations by Zhang et al. (2007) from the VLA archive and found that the discrepancy is mainly due to different weighting schemes used in the imaging; i.e., our 7 mm image was created with natural weighting to improve the signal-to-noise ratio, whereas Zhang et al. (2007) apparently used a more uniform weighting scheme, given that they have data with a better sensitivity. For example, if our data are imaged using a Briggs' robust parameter of 0, then the peak intensity of the 7 mm source is 1.0 mJy beam^{-1} (i.e., the same value reported by Zhang et al. 2007) and the integrated flux density is 2.6 ± 0.6 mJy. Our reduction of the Zhang et al. data using a robust 0 weighting resulted in an integrated flux density of 1.74 ± 0.35 mJy—i.e., we reproduced the value reported by Zhang et al. (2007)—and the flux density is consistent within the errors with the corresponding flux density derived from our data. Regarding the size and position angle, given the low signal-to-noise ratio of both data sets, and that the 7 mm source is barely resolved, it is difficult to accurately measure the deconvolved size and position angle of the source. However, for example, if a robust 0 weighting is used in the imaging of the Zhang et al. (2007) data, we found that the maximum size of the 7 mm source is $3.7'' \times 1.7''$, with a position angle of 44°, which is consistent with our results (Table 2). Higher sensitivity and angular resolution observations are needed to precisely measure the size and position angle of the 7 mm source. Nevertheless, our observations and those of Zhang et al. (2007) are consistent with an elongated source almost perpendicular to the ionized jet that we report in this work.

Zhang et al. (2007) also conducted VLA continuum observations at 22 GHz and found no radio continuum emission at a 1 σ level of 0.14 mJy beam^{-1}. They also pointed out that Miralles et al. (1994) did not detect 2 cm emission at a 1 σ level of 0.16 mJy, whereas Araya et al. (2005) report a 0.7 mJy source at 2 cm. Zhang et al. (2007) mentioned that variability of the radio continuum emission in the source may be responsible for this apparent discrepancy. We note that Miralles et al. (1994) did not consider a 1 σ value as an appropriate detection limit for the radio continuum, but they report upper limits of ≤ 0.5 and ≤ 0.8 mJy for 6 cm and 2 cm emission that are consistent with our 6 cm detection (Table 2) and the 2 cm detection by Araya et al. (2005). Regarding the nondetection of 22 GHz emission reported by Zhang et al. (2007), the 5 σ detection limit of their data is 0.7 mJy beam^{-1}, and the peak intensity of the 22 GHz source reported in this work (see Fig. 1) is 0.65 mJy beam^{-1}; i.e., at a 5 σ detection limit, the two data sets are consistent. The nonlinear nature of interferometric observations, particularly at the K band, where tropospheric instabilities may lead to phase decorrelation, can be responsible for the nondetection of the source at a 5 σ level. Thus, given the available radio continuum data, we find no strong evidence for variability of the source. Nevertheless, the occurrence of flares in the H_2CO maser (Araya et al. 2007c; see also Araya et al. 2007a) may be caused by variability of the radio continuum; thus, future observations are required to investigate whether, and up to what level, the radio continuum emission is variable in this source.

3.3.3. *Mass Determination*

On the basis of the millimeter- and submillimeter-wavelength data, Zhang et al. (2007) report a spectral index α of 3.9 ($S_\nu \propto \nu^\alpha$) and thus an emissivity index of $\beta = 1.9$, which is consistent with the value of $\beta = 1.8$ derived from theoretical, as well as empirical,

considerations (see § 3.1). However, in an effort to better constrain the value of β by matching beam sizes, Zhang et al. (2007) derived a value of $\beta = 1.3$, which they believe to be more appropriate for the dust mass determination. On the basis of NH_3 observations, they obtained a kinetic temperature of 80 K for the molecular core associated with the 7 mm source, which was assumed to be the dust temperature. In addition, they assumed an opacity of $\kappa(250\ \mu\mathrm{m}) = 12\ \mathrm{cm^2\ g^{-1}}$. Using these parameters, Zhang et al. (2007) estimated a mass of 70 $M_\odot$ within 30,000 AU from the 7 mm source. Using the same parameters [$T_d = 80$ K, $\kappa(250\ \mu\mathrm{m}) = 12\ \mathrm{cm^2\ g^{-1}}$, and $\beta = 1.3$], we derive a mass of $\sim$80 $M_\odot$ on the basis of our observations. Given the flux density uncertainties (Table 2), our derived mass is consistent with the 70 $M_\odot$ mass reported by Zhang et al. (2007).

3.3.4. *A Molecular Core Coincident with the Torus Candidate*

Zhang et al. (2007) detected compact molecular emission from the position of the torus candidate in their NH_3 and HCN observations. As mentioned above, the NH_3 emission at the position of the 7 mm source traces warm ($\sim$80 K) material, and in addition, the line width of the NH_3 emission is substantially broader (FWHM = 8.7 km s^{-1}) when compared to the more extended NH_3 emission (FWHM $<$ 2 km s^{-1}). Zhang et al. (2007) find it unlikely that the broad line width is due to the outflow; instead, the large line width may be due to relative motion of multiple cores, or due to infall/rotation. They found that if rotation is assumed, then the dynamical mass (assuming gravitationally bound motion) would be similar to the 70 $M_\odot$ mass reported by Zhang et al. (2007; see also § 3.3.3). However, their data do not show direct kinematic evidence for rotation of the core.

The peak velocity of the NH_3 emission is 85.2 km s^{-1}, which closely agrees with the systemic velocity of the source as traced by CS emission and H_2CO absorption (Bronfman et al. 1996; Araya et al. 2004). The local standard of rest velocity of the H_2CO maser in the region is $\sim$80 km s^{-1}; thus, the maser is not tracing gas at the systemic velocity of the molecular core, but is tracing blueshifted material, perhaps associated with the base of the molecular outflow or a flaring disk with radial velocity gradients.

4. SUMMARY

We report 6 cm, 3.6 cm, 1.3 cm, and 7 mm observations of IRAS 18566+0408 conducted with the VLA. We detected radio continuum emission from the source at all wavelengths. The centimeter emission appears to trace an ionized jet, whereas the 7 mm band is dominated by thermal dust emission. The interpretation that the centimeter radiation arises from an ionized jet is strengthened by *Spitzer* IRAC observations of IRAS 18566+0408 that show excess at 4.5 μm at the same orientation as the suggested ionized jet.

The 7 mm structure is elongated almost perpendicular to the ionized jet. If we take into account that the 7 mm emission is dominated by thermal dust, then the 7 mm source appears to trace a circumstellar torus. The mass of the torus-like structure is greater than 10 $M_\odot$ (and as large as several hundred solar masses, depending on the assumed dust opacity and temperature). Given that definitive identification of a disk or torus requires kinematical evidence of rotation, future subarcsecond angular resolution molecular line observations are required to confirm the torus interpretation presented in this paper.

Our results are consistent with recent molecular and continuum observations reported by Zhang et al. (2007). They found a SiO outflow that is approximately parallel to the ionized jet reported in this work, as well as a clump of NH_3 and HCN molecular gas at the position of the torus-like structure. Zhang et al. (2007) also conducted 7 mm VLA observations of the region and found an elongated structure whose orientation is almost perpendicular to the ionized jet reported in this work, which confirms our 7 mm results.

The H_2CO 6 cm maser in IRAS 18566+0408 (Araya et al. 2005) is coincident with the center of a torus-like structure that harbors a massive protostellar candidate. This result strengthens the association of H_2CO 6 cm masers with very young massive stellar objects. The observed radio spectral energy distribution rules out pumping of the H_2CO 6 cm maser in IRAS 18566+0408 by radio continuum, which Boland & de Jong (1981) proposed as the excitation mechanism for the H_2CO maser in NGC 7538.

E. A. is supported by a NRAO predoctoral fellowship. P. H. acknowledges support from NSF grant AST 04-54665. H. L. was supported by a postdoctoral stipend from the German Max Planck Society. E. C. and M. S. were supported in part by NSF grant AST 03-03689. L. O. was supported in part by the Puerto Rico Space Grant Consortium. G. G. acknowledges support from FONDAP project 15010003. We thank an anonymous referee for comments that improved the manuscript. This research has made use of NASA's Astrophysics Data System and is based in part on observations made with the *Spitzer Space Telescope*, which is operated by the Jet Propulsion Laboratory, California Institute of Technology, under contract with NASA.

REFERENCES

Araya, E., Hofner, P., & Goss, W. M. 2007a, in IAU Symp. 242, Astrophysical Masers and Their Environments, ed. J. Chapman & W. A. Baan (Cambridge: Cambridge Univ. Press), in press (arXiv: 0707.1841v1)
Araya, E., Hofner, P., Goss, W. M., Kurtz, S., Linz, H., & Olmi, L. 2006, ApJ, 643, L33
Araya, E., Hofner, P., Goss, W. M., Linz, H., Kurtz, S., & Olmi, L. 2007b, ApJS, 170, 152
Araya, E., Hofner, P., Kurtz, S., Linz, H., Olmi, L., Sewiło, M., Watson, C., & Churchwell, E. 2005, ApJ, 618, 339
Araya, E., Hofner, P., Linz, H., Sewiło, M., Watson, C., Churchwell, E., Olmi, L., & Kurtz, S. 2004, ApJS, 154, 579
Araya, E., Hofner, P., Sewiło, M., Linz, H., Kurtz, S., Olmi, L., Watson, C., & Churchwell, E. 2007c, ApJ, 654, L95
Arce, H. G., Shepherd, D., Gueth, F., Lee, C.-F., Bachiller, R., Rosen, A., & Beuther, H. 2007, in Protostars & Planets V, ed. B. Reipurth, D. Jewitt, & K. Keil (Tucson: Univ. Arizona Press), 245
Beltrán, M. T., Cesaroni, R., Codella, C., Testi, L., Furuya, R. S., & Olmi, L. 2006, Nature, 443, 427
Beuther, H., Churchwell, E. B., McKee, C. F., & Tan, J. C. 2007, in Protostars & Planets V, ed. B. Reipurth, D. Jewitt, & K. Keil (Tucson: Univ. Arizona Press), 165
Beuther, H., Schilke, P., Sridharan, T. K., Menten, K. M., Walmsley, C. M., & Wyrowski, F. 2002a, A&A, 383, 892
Beuther, H., Walsh, A., Schilke, P., Sridharan, T. K., Menten, K. M., & Wyrowski, F. 2002b, A&A, 390, 289
Boland, W., & de Jong, T. 1981, A&A, 98, 149
Bronfman, L., Nyman, L.-Å., & May, J. 1996, A&AS, 115, 81
Carral, P., Kurtz, S., Rodríguez, L. F., Martí, J., Lizano, S., & Osorio, M. 1999, Rev. Mex. AA, 35, 97
Cesaroni, R., Galli, D., Lodato, G., Walmsley, C. M., & Zhang, Q. 2007, in Protostars & Planets V, ed. B. Reipurth, D. Jewitt, & K. Keil (Tucson: Univ. Arizona Press), 197
Churchwell, E. 2002, ARA&A, 40, 27
Fish, V. L. 2007, in IAU Symp. 242, Astrophysical Masers and Their Environments, ed. J. Chapman & W. A. Baan (Cambridge: Cambridge Univ. Press), in press (arXiv:0704.0242v1)

Forster, J. R., Goss, W. M., Gardner, F. F., & Stewart, R. T. 1985, MNRAS, 216, P35
Garay, G., Brooks, K., Mardones, D., & Norris, R. P. 2003, ApJ, 587, 739
Garay, G., et al. 2007, A&A, 463, 217
Hill, T., Thompson, M. A., Burton, M. G., Walsh, A. J., Minier, V., Cunningham, M. R., & Pierce-Price, D. 2006, MNRAS, 368, 1223
Hoffman, I. M., Goss, W. M., & Palmer, P. 2007, ApJ, 654, 971
Hoffman, I. M., Goss, W. M., Palmer, P., & Richards, A. M. S. 2003, ApJ, 598, 1061
Litvak, M. M. 1970, ApJ, 160, L133
Martí, J., Rodríguez, L. F., & Reipurth, B. 1995, ApJ, 449, 184
Mehringer, D. M., Goss, W. M., & Palmer, P. 1995, ApJ, 452, 304
Miralles, M. P., Rodríguez, L. F., & Scalise, E. 1994, ApJS, 92, 173
Molinari, S., Brand, J., Cesaroni, R., & Palla, F. 1996, A&A, 308, 573
Noriega-Crespo, A., et al. 2004, ApJS, 154, 352
Ossenkopf, V., & Henning, Th. 1994, A&A, 291, 943
Pratap, P., Menten, K. M., & Snyder, L. E. 1994, ApJ, 430, L129
Reynolds, S. P. 1986, ApJ, 304, 713
Rodríguez, L. F., Zapata, L. A., & Ho, P. T. P. 2007, ApJ, 654, L143
Rodríguez, L. F., et al. 1998, Nature, 395, 355
Smith, H. A., Hora, J. L., Marengo, M., & Pipher, J. L. 2006, ApJ, 645, 1264
Sridharan, T. K., Beuther, H., Schilke, P., Menten, K. M., & Wyrowski, F. 2002, ApJ, 566, 931
Thaddeus, P. 1972, ApJ, 173, 317
Zhang, Q. 2005, in IAU Symp. 227, Massive Star Birth: A Crossroads of Astrophysics, ed. R. Cesaroni, M. Felli, E. Churchwell, & M. Walmsley (Cambridge: Cambridge Univ. Press), 135
Zhang, Q., Sridharan, T. K., Hunter, T. R., Chen, Y., Beuther, H., & Wyrowski, F. 2007, A&A, 470, 269